CELLULAR AUTOMATON MODELLING OF SLAB AVALANCHE TRIGGERING MECHANISMS: FROM THE UNIVERSAL STATISTICAL BEHAVIOUR TO PARTICULAR CASES

J. Faillettaz[1], F. Louchet[2*] & J-R. Grasso[3]

[1] Laboratoire 3S, Grenoble, France. *Present address*: VAW ETH-Zurich, Switzerland,
[2] Laboratoire de Glaciologie et de Géophysique de l'Environnement, Grenoble, France
[3] Laboratoire de Géophysique Interne et de Tectonophysique, Grenoble, France

ABSTRACT: Modelling avalanche release is a long lasting challenge. Despite a general agreement on the basic mechanisms responsible for avalanche release, deterministic models suffer from a lack of reliable data due to spatial and temporal variability of snow cover properties. On the other hand, field observations reveal that starting zone sizes are organized into power law statistical distributions characterized by a universal exponent. Yet, statistical approaches developed so far, that essentially are binary cellular automata, only consider the shear failure of the weak layer, and cannot take into account slab rupture. As a consequence, they cannot reproduce the observed power law exponent. This is why the present model is a two-threshold multi-state cellular automaton, that incorporates both the shear failure of the weak layer and the rupture of the slab. It reproduces field data on statistical distributions of starting zones of snow slab avalanches, but also of other gravitational failures. It can be used to model blast-triggered and skier triggered avalanche, or to provide initial conditions in avalanche flow simulations in particular slopes. Possible applications of the automaton to educational purposes may be contemplated.

KEYWORDS: snow, avalanches, cellular automata, statistical physics, variability, criticality.

1. INTRODUCTION

Avalanche starting zones sizes is a key information used as an input in simulations of avalanche flow. It can be characterized by both the width L (or the area L^2) of the starting zone and by the slab depth H. These parameters that are intimately linked to the details of the triggering mechanisms, are known to be highly variable. In contrast with a current belief, a careful statistical analysis [Faillettaz (2003), Faillettaz et al.(2002)] showed that H and L values were not correlated, as illustrated in Figure 1: avalanches with a given depth H can display a wide range of L values, and conversely. However, despite such an apparent randomness, values retrieved from field measurements were shown to exhibit so-called scale-invariant statistics, i.e. to obey well defined power law distributions [Louchet et al. (2002)], $N(L) \propto L^{-b}$ and $N(H) \propto H^{-b'}$ where N(L) and N(H) are the number of avalanches of width L and of depth H (see Figure 2). Despite the fact that H and L values are not correlated, the exponents of the corresponding power law distributions are very close to each other: $b \approx b' = 3.4 \pm 0.1$ for probability distribution functions of lengths (i.e. non cumulative distributions), corresponding to 2.4 for cumulative length distributions. Interestingly, all available avalanche data align on the same power law, whatever the winter season, the mountain range, or the gully they start from. Such a "universal" character is remarkable, suggesting a common and quite general explanation.

* *Corresponding author address:* Francois Louchet, Laboratoire de Glaciologie et de Géophysique de l'Environnement, UJF/CNRS, BP96 – 38402 Saint Martin d'Hères (F), tel: +33 4 76 82 42 51, email: louchet@lgge.obs.ujf-grenoble.fr

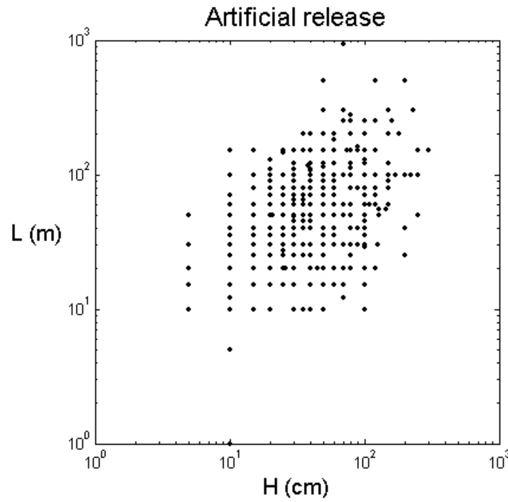

Figure 1: H vs L values for 3450 avalanches, recorded in La Plagne and Tignes ski resorts. Each single point corresponds to one or several avalanches.

Numerous studies were undertaken on the basis of numerical simulations [Bak et al. (1988), Hergarten (2002), Nuñez Amaral and Lauritsen (1997), Olami et al. (1992), Sornette (2000), Vespignani and Zapperi (1998), Hergarten and Neugebauer (2000), Densmore et al. (1998)] to understand the origin of this scale invariance and the value of the scaling exponent of widths (L) or areas (L^2) distributions. Such approaches, based on Bak's sand pile model, qualitatively reproduce the observed scaling behaviour. However, the exponents do not usually agree with observations, except if other ingredients (dissipation, heterogeneities, or any tuning parameter) are introduced.

This was also the case of our first cellular automaton [Faillettaz et al. (2004)] in which cells were found in two possible states (non-damaged (0) or damaged (1)), depending on whether the load experienced by a given cell was respectively smaller or larger than a given shear threshold characteristic of the weak layer strength. The mechanics of basal crack growth was taken into account through load transfers between a damaged cell and its non-damaged first neighbours, that may in turn change the state of some of the neighbour cells, and so forth. This model reproduced the scale invariant size distribution of avalanches. However, the power law exponent did not match field observations, the main reason being that, owing to the binary character of the automaton, the weak layer

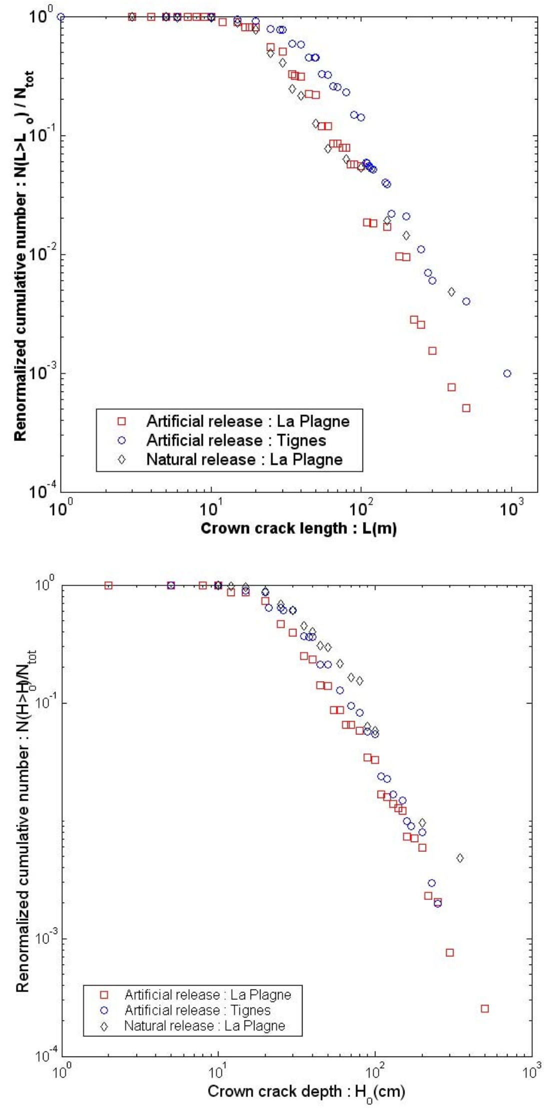

Figure 2: Cumulative length distributions for L and H, retrieved from both artificial and natural triggerings (La Plagne and Tignes ski resorts), giving a similar exponent of 2.4

failure was the only one to be taken into account through a single failure threshold, and crown crack opening could not be considered.

This is the reason why a more sophisticated cellular automaton was developed, in which each cell state could take a continuous value between 0 (undamaged) to τ_0 (totally damaged in shear). This improvement allowed the introduction of a second threshold, corresponding to slab failure, in order to better take into account the two basic steps involved in slab avalanche triggering. The first results [Faillettaz et al.

(2002)] nicely reproduced the features of slab avalanches, in which a well defined starting zone was clearly evidenced, triggering in turn downslope a triangle-shaped long range cascading cell failure zone. The model reproduced scale invariant size distributions only if some randomness was introduced in slab rupture thresholds [Faillettaz (2003)]. In more recent developments [Faillettaz et al. (2004)] it was shown to reproduce field observations (and more particularly the measured power law exponent values), and to apply not only to slab avalanches, but also to other gravitational failures.

After a summary of the last results obtained by this simulation, the present paper discusses possible applications of the model to the understanding of artificial triggerings, and to avalanche risk evaluation.

2. THE MODEL

Slab release can be described as a first approximation by the succession of four main steps [Louchet and Duclos (2006)]: i) nucleation of a basal crack, ii) expansion of the basal crack, iii) nucleation of a crown crack, and iv) expansion of the crown crack. Simple calculations can be made on this basis within the assumption of a shear disturbance in the weak layer separating an homogeneous slab from an homogeneous substrate [e.g. McClung (1981), Louchet (2001)]. Despite interesting qualitative results, such simplified approaches cannot predict avalanche sizes, owing to the large variability of the snowpack properties.

The present model is a typical statistical physics approach. The spatial variability of snow properties is taken into account through the introduction of randomness in a discretized 2-d network mimicking the weak layer. The model incorporates the physics of triggering through the use of two different failure modes, corresponding to two different failure thresholds: a first one for the weak layer shear failure, that controls both basal crack nucleation and expansion, and another one for slab failure, that controls crown crack nucleation and expansion.

The proximity to failure of a given cell is defined by a single variable ζ_i, that can take continuous values, from 0 to τ_0, i.e. from undamaged to totally failed. Periodic boundary conditions are taken in the horizontal direction. The automaton may be run in different ways, giving equivalent results. For instance, it may be initialized to zero (i.e. totally undamaged). In this case, during each run, load increments $\Delta\zeta$ are scattered at random on the network. A given shear threshold value τ_0 is taken for each run. A given cell fails in shear when its ζ_i value exceeds the threshold value, which brings the ζ_i value back to zero. The excess ζ_i value (as well as further load increments) is then equally redistributed onto its unfailed first neighbours (i.e. the simulation is "conservative").

A failure of the second type occurs between a cell i and one of its neighbours j (located above or aside the considered cell) when the difference $||\zeta_i-\zeta_j||$ exceeds a slab rupture threshold σ_0. In this case, the two involved cells are no more considered as neighbours, and redistribution of excess load between these cells becomes forbidden. As a consequence of load redistribution rules, the model is polarised, i.e. the x and y directions have different behaviours, which simulates the slope direction. A peculiarity of our model relative to other avalanche or sandpile simulations [references in part 1, Fyffe and Zaiser (2004), Kronholm and Birkeland (2005)] is that, in close agreement with the mechanics of snow slab failures, we introduced a second failure mode controlled by a finite slab strength threshold. The basal shear failure controls indeed the avalanche occurrence, whereas the slab rupture controls the avalanche size.

Another difference with previous studies is that the simulation is conservative, i.e. there is no healing on a broken cell. In such a stress-driven simulation, the system is ineluctably brought to a final macroscopic instability, defined as the stage at which a macroscopic shear failure (labelled MS in the following, for "macroscopic shear event") occurs and expands up to the system size. We observe in our simulations that every time a MS event occurs, a remaining "C-cluster" remains within the MS cluster, that is made of cells that are still unbroken in terms of slab rupture (e.g. see figure 5). By analogy with the failure patterns observed in the field, we choose the size of the unbroken C-cluster as the relevant parameter to measure the size of the triggering zone. We checked that this measure is not affected by the finite size of the system. By contrast, the MS event simulates the cascading effect induced by the initial snow slab failure, and is not considered here.

The system is reinitialised before each run taking a new strength threshold at random from a uniform distribution in an interval between $\Delta\zeta$ and the slab threshold σ_0. Picking up the size of the C-cluster for each run from thousands of runs leads to power law distributions of slab failure sizes (figure 3). Among these runs, those with small slab thresholds correspond to small starting zones.

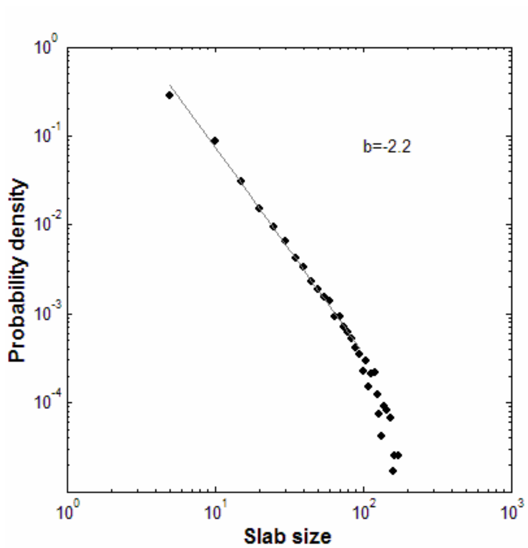

Figure 3: Distribution of avalanche sizes obtained from the cellular automaton with α_{max}=0.5 (see text), reproducing avalanche field data.

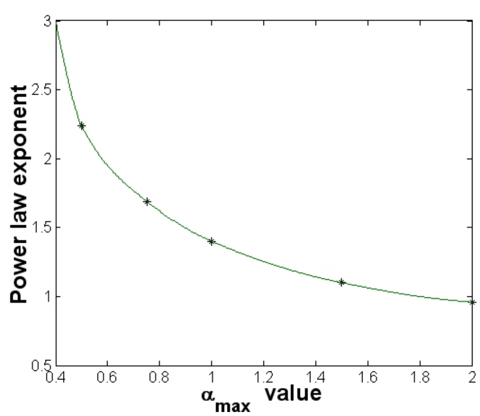

Figure 4: Influence of α_{max} on the value of the power law exponent. The exponent value for snow avalanche non-cumulative area distributions (i.e. probability distribution functions) b = 2.2 correspond to $\alpha_{max} \approx 0.5$.

The power law exponents given by the automaton can be varied by tuning a single parameter, defined by α_{max}=max[σ_0/τ_0], i.e. the maximum value of the ratio of slab rupture to weak layer shear failure thresholds, that characterises the strength distribution from which the slab failure threshold is taken at random at each run. This parameter is a possible measure of the cohesive anisotropy of the material. A number of other gravitational failures also obey a power law distribution. By tuning α_{max}, the range of observed values for the scaling exponents of these systems can be reproduced (figure 4). The exponent value of 2.2, characteristic of slab avalanche non-cumulative area distributions (corresponding to exponents of 3.4 $\pm$ 0.1 for probability distribution functions of widths L, and 2.4 for cumulative distributions of widths L, as shown in figure 2), is obtained for α_{max} =0.45 to 0.55, which lies between those for landslides and for rockfalls [Dussauge et al. 2003, Rothman et al. 1994]. Such α_{max} values allow an inverse estimation of the respective anisotropies of the involved materials. α_{max} values close to unity correspond to isotropic materials, suggesting that the more layered the material is, the smaller the α_{max} value, i.e. the larger the b value. In other words, the more layered the material is, the more numerous the small starting zones as compared to the big ones. Rockfalls correspond to $\alpha_{max}\approx 0.8$, favouring large sized events, whereas the value for landslides is of about 0.3 to 0.4, probably due to a strong tendency for strain softening.

For the simple geometry of slab avalanches, α_{max} <1 suggests a slab strength smaller than the basal shear resistance. This finding seems at first glance to contradict the "general" agreement that crown crack opening is a consequence of a relatively easier basal failure. The answer is twofold:

i) On the field, the roughness of the shear surface, possible defect healing, and the presence of anchoring points make the macroscopic shearing process more difficult than what occurs during laboratory shear tests. Such effects have no influence on slab failure initiation, as it essentially occurs in tension, except for "anchoring points" (trees, outcrops) that may by contrast facilitate crown crack opening.

ii) The snow cover experiences a particular loading mode: the weak layer experiences the whole downhill component of the snow weight, whereas tensile stresses responsible for crown crack opening only arise from stress gradients (this is the reason why crown crack opening is controlled in our automaton by the difference in ζ values between two neighbour cells). These differential slab stresses are usually much smaller than shear stresses acting on basal planes, and our finding that the right power law exponent is found when the corresponding threshold is smaller than that for basal failure is not surprising.

3. APPLICATION TO ARTIFICIALLY TRIGGERED AVALANCHES

The automaton described above reproduces the scale-free distribution of natural avalanches: the variations of the parameter ζ_i may indeed represent either the local load increase on a cell due to a snowfall, or the decrease of the weak layer strength due to metamorphism. The same automaton can also be used to simulate avalanches on particular paths, introducing slope changes through local changes in shear and slab failure thresholds, keeping the α_{max} value constant. Such "personalised" simulations, after some parameter calibration in order to fit available field data of a given avalanche site, may be run thousands of times. This procedure would provide to avalanche flow simulations trustable initial conditions, equivalent to those that would have required thousands of years of field measurements

It may also simulate blast triggered or skier-triggered avalanches. For this purpose, a group of cells can be artificially damaged around the blast location, or along the skier's trajectory.

An example of several skiers gliding down a reasonably safe slope (dark and pale blue cells only) is shown in Figure 5. The skier's weight is negligible as compared to that of the slab, but the local pressure under the skis may locally collapse the weak layer. In the simulation, the system is initialized randomly. The additional damage due to the skier is performed by an increase of the ζ_i value by one $\Delta\zeta_i$ increment on each cell on which the skier actually travels. This damage may spontaneously extend through a "domino effect".

It can be easily imagined that a given trajectory taken at random may entirely cross the system without any avalanche release if the skier is lucky enough not to cross areas that are already significantly damaged. But another path, possibly very close to the previous one, may result in a sudden triggering. In the present case, the cells on each skier trajectory turn from dark blue to green, or from pale blue to yellow. Some of them may turn to yellow or red due to a "domino effect". Slab release takes place when a fourth skier crosses the (already damaged) trajectory of a previous one: an incipient cluster of red cells form, that readily expands and trigger a large scale instability.

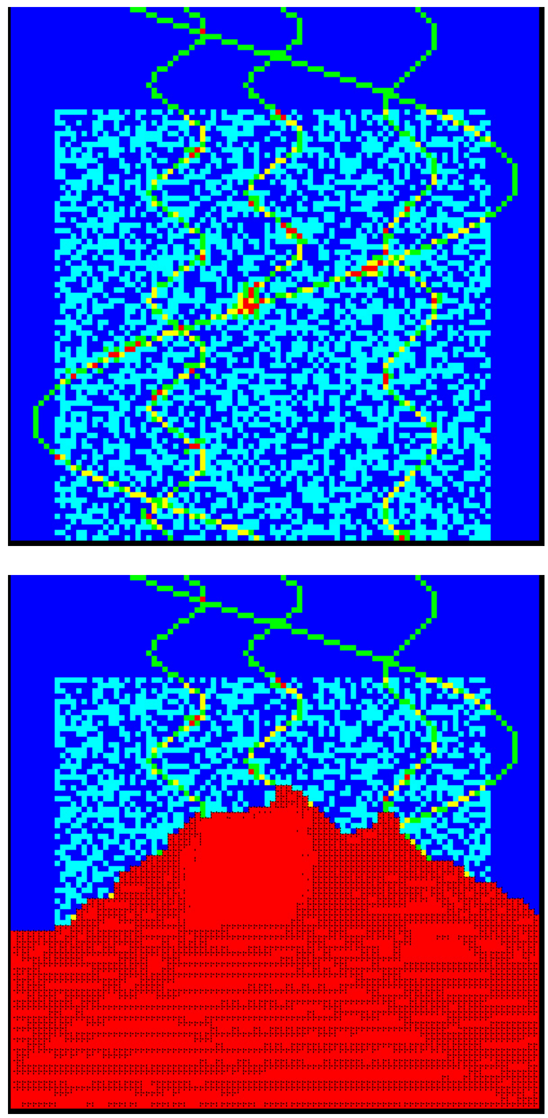

Figure 5: Avalanche triggered by several skiers. The avalanche starts in the vicinity of the crossing between the large amplitude track (that could represent the skier climbing track) and the central one (downhill track).

In order to take into account the fact that, on stiffer slabs, the damage may extend at some distance away from the skier's path, the damage rule can be modified: instead of damaging the cells on which the skier actually travels, the direct damage produced by the skier is extended to further neighbour cells. An avalanche may then be released if the damaged zones overlap, even if the skiers trajectories had not crossed each other (see Figure 6).

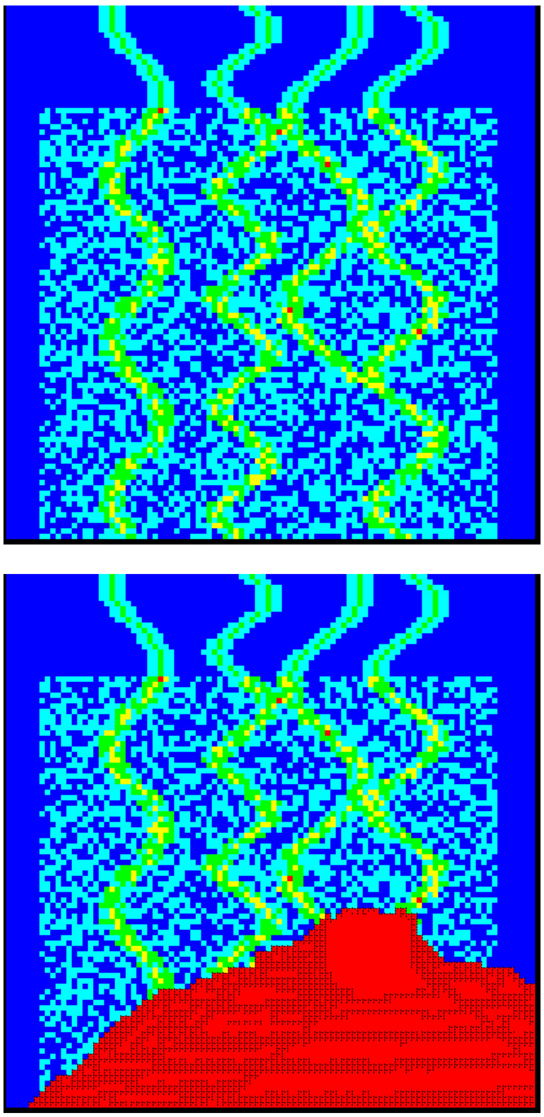

Figure 6: Example in which the direct damage produced by the skier is extended to further neighbour cells (here 3 cells). In this particular case, an avalanche is released even if the skier downhill tracks had not crossed each other.

4. SUMMARY AND CONCLUSION

The present 2-dimensional 2-threshold cellular automaton incorporates at the local scale the physics of weak layer and slab failure mechanisms through two specific failure thresholds. The basal shear failure controls the avalanche occurrence, whereas the slab rupture controls the avalanche size. The system spatial variability is accounted for through the discretization of the network and the random character of loading. The temporal variability is introduced in terms of random changes of failure thresholds at each run. The automaton contains a single physically-based tuning parameter, related to the failure strength anisotropy of the material. It reproduces the scale-invariant size distributions of slab avalanches starting zones, but also of other gravitational failures, through slight variations of this parameter.
This automaton can now be used to simulate avalanche release in various particular cases. The influence of various parameters on blast-triggered and skier triggered avalanches can be investigated on this basis, mimicking the effects of blast pressure or extension, or those of slab depth and stiffness through the local damage extension and strength, as shown here in the case of skier-triggered avalanches. It may also be used to provide initial conditions in avalanche flow simulations in particular slopes. Possible applications of the automaton to educational purposes may be contemplated.

REFERENCES:

Bak P., Tang C. and Wiesenfeld K., 1988. Self organised criticality Phys. Rev. A 38, 364.

Densmore A. L. et al., 1998. Landsliding and the evolution of normal-fault-bounded mountains J. Geophys. Research 103, 15203.

Dussauge C., Grasso J.R. and Helmstetter A. 2003. Statistical analysis of rockfall volume distributions: Implication for rockfall dynamics. J. Geophys. Res. 108(B6), 2286.

Faillettaz J, Louchet F. and Grasso J.R. 2004. Two-threshold model for scaling laws of non interacting snow avalanches, Phys. Rev. Letters 93, 208001.

Faillettaz J., Louchet F., Grasso J-R., Daudon D., and Dendievel R., 2002. Scale invariance of snow triggering mechanisms. Proc. ISSW, 528.

Faillettaz J., Louchet F., Grasso J-R. 2003. Possible reasons for the scale invariance of avalanche starting zone sizes. International Glaciological Society meeting, Davos (CH).

Faillettaz J., 2003. Le déclenchement des avalanches de plaque de neige : de l'approche mécanique à l'approche statistique. PhD thesis, Institut National Polytechnique de Grenoble.

Fyffe B. and Zaiser M., 2004. The effects of snow variability on slab avalanche release, Cold Reg. Sci. Technol., 40, 229-242.

Hergarten S. and Neugebauer H., 2000. Self-organized criticality in two-variable models J. Phys. Rev. E 61, 2382.

Hergarten S., 2002. Self-Organized Criticality in Earth Systems (Springer Verlag, Berlin, Heidelberg).

Kronholm K. and Birkeland K.W., 2005. Integrating spatial patterns into a snow avalanche cellular automata model, Geophys. Res. Lett. 32, L19504.

Louchet F. and Duclos A., 2006 Insight into slab-avalanche triggering. A combination of four phenomena in series. The Avalanche Review, Vol. 24, no 3, (the American Avalanche Association Inc.),

Louchet F. and Duclos A., this conference

Louchet F., 2001. A transition in dry snow slab avalanches triggering modes Annals of Glaciology, 32, 285.

Louchet F., Faillettaz J., Daudon D., Bédouin N., Collet E., Lhuissier J. and Portal A-M., 2002. Possible deviations from Griffith's criterion in shallow slabs and consequences on slab avalanche release. Natural Hazards and Earth System Sciences, vol. 2, nb 3-4.

McClung D.M., 1981. Fracture mechanical models of dry slab avalanche release. J. Geophys. Res. 86, B11, 10783.

Nuñez Amaral L.A. and Lauritsen K.B., 1997. University classes for rice-pile models. Phys. Rev. E 56, 231.

Olami Z., Feder H.J.S., and Christensen K., 1992. Self-organized criticality in a continuous, nonconservative cellular automaton modeling earthquakes Phys. Rev. Letters 68, 1244.

Rothman D.H., Grotzinger J.P., and Flemings P., 1994. Scaling in turbidite deposition. J. Sedim. Research, Sect. A, A64, 59.

Sornette D., 2000. Critical Phenomena in Natural Sciences (Springer, New York).

Vespignani A. and Zapperi S., 1998. How self-organized criticality works : A unified mean-field picture Phys. Rev. E 57, 6345.